

Analyzing Communicability and Connectivity in the Indian Stock Market During Crises

PAWANESH PAWANESH*

*Department of Mathematics, Shiv Nadar Institution of Eminence Deemed to be University,
Dadri, Gautam Buddha Nagar, Uttar Pradesh, India*

*Corresponding author: py506@snu.edu.in

CHARU SHARMA

*Department of Mathematics, Shiv Nadar Institution of Eminence Deemed to be University,
Dadri, Gautam Buddha Nagar, Uttar Pradesh, India*

AND

NITEESH SAHNI

*Department of Mathematics, Shiv Nadar Institution of Eminence Deemed to be University,
Dadri, Gautam Buddha Nagar, Uttar Pradesh, India*

[Received on 13 February 2025]

In financial networks, information does not always follow the shortest path between two nodes but may also take alternate routes. Communicability, a network measure, resolves this complexity and, in diffusion-like processes, provides a reliable measure of the ease with which information flows between nodes. As a result, communicability appears to be an important measure for detecting disturbances in connectivity within financial systems, similar to instability caused by periods of high volatility. This study investigates the evolution of communicability measures in the stock networks during periods of crises, showing how systemic shocks strengthen the pairwise interdependence between stocks in the financial network. In this study, the permutation test reveals that approximately 83.5 % of stock pairs were found to be statistically significant at the significance level of 0.001 and have an increase in the shortest communicability path length during the crisis than the normal days, indicating enhanced interdependence and heightened information-flow in the market. Furthermore, we show that when employed as features in the classification model, the network's shortest path-based measures, along with communicability measures, are able to accurately classify between the times periods of market stability and volatility. Additionally, our results show that the geometric measures perform better in terms of classification accuracy than topology-based measures. These findings provide important insights into market behaviour during times of increased volatility and advance our understanding of financial market crises.

Keywords: Financial network analysis, Complex network, Communicability measure, Support vector machine

1. Introduction

The financial system is widely regarded as one of the most complex systems. At its most fundamental structural level, the global financial network is made up of billions of individual transactions and organizations, including traders, institutions, and markets, that communicate via financial instruments

and market interactions. These entities are linked together within localized institutions, such as regional financial markets or sectors, and then aggregated into bigger systems, such as the global stock exchange. Researchers are studying this system using methods and tools from across fields to help better understand and advance economic growth and development, policy-making and regulation, risk management and sustainability, technological advancement and innovation. In the recent past, modelling a financial system as an interconnected node has been a popular approach. In particular, complex networks have emerged as a powerful tool for better modelling the pairwise interaction between financial entities such as stocks, cryptocurrency, and bonds. Many researchers have modelled the pairwise correlations between daily logarithmic returns of stocks to construct the networks. Kendall's tau and mutual information measures have also been widely used to model the interaction between stock pairs. A huge amount of literature leverages the topology as well as the geometry of these financial networks [1, 13, 17, 18, 24, 28, 32, 33, 35, 37]. In a similar line, Several authors have used traditional network metrics such as Eigenvector centrality, betweenness centrality, degree centrality, and hybrid centrality measures to study these financial networks with the aim of proposing portfolio selection strategies, risk management, and uncovering hidden patterns in stock market dynamics [1, 17, 30, 34, 40].

In the past literature, it has been observed that the study, prediction, and identification of market stability and volatility periods have been crucial topics of research in financial Markets. Many authors have studied and focused on the correlation matrix of stock returns and captured the market turbulence periods [3, 11, 25, 39]. Furthermore, several authors have used network theory tools on the correlation matrix to detect and predict the stock market crisis periods [19, 20, 36, 41]. In the year 2020, Vishwas Kukreti et al. [19] studied the correlation-based networks and used recently developed entropy measures, such as structural entropy and eigen entropy and showed how entropy measures could be used to identify normal, bubble, and crash periods. In the same year, 2020, Kulkarni et al. [20] studied the correlation-based network of stocks comprising the National Stock Exchange (NSE) and the Bombay Stock Exchange (BSE) using geometry-inspired measures of network and captured the crisis periods of Indian stock market. Specifically, they monitored the changes occurring in the two Indian stock markets by analyzing the fluctuations in standard network measures, discrete Ricci curvatures, and persistent homology-based topological measures. As we mentioned earlier, several network metrics are well-documented in the literature, and many of them were used to study financial networks and propose a deeper understanding of the system.

Thus, according to the literature discussed above, network metrics have been crucial tools for investigating these challenges over the full cross-correlation matrix as well as over the correlation-based network. When working with the network's shortest path-based approaches, the authors primarily explored traditional network measures, yet limited conclusive results were reached. It would be very interesting to investigate the potential of alternative, unconventional network metrics as novel and effective in distinguishing periods of market stability and volatility. we know that stock networks are more connected during times of crisis, indicating larger linkages between equities as market dynamics change. This is frequently caused by panic selling, elevated volatility, and the spread of systemic risk.

In the recent literature, we have observed the application of the communicability measure of the networks in the field of biology and world trade networks [22, 23]. Thus, communicability is a broader measure of connectedness that seeks to quantify the ease of communication between two nodes by considering not only the shortest path but all conceivable paths linking them [9, 12]. This measure indicates the network property of information to flow under a diffusion model: as a result, it could be particularly suited to studying the turbulence periods networks; also, it may be highly sensitive. In the year 2019, Lella et al. [22] used the communicability measure to study the disruption of connectivity among brain

regions caused by white matter degeneration due to Alzheimer's disease. Similarly, in 2020, Lella and Estrada [23] used the communicability distance to reveal the hidden pattern in patients with Alzheimer's disease. First, they show that the shortest communicability path length performs noticeably better than the shortest topological path length in distinguishing between people with Alzheimer's disease (AD) and healthy persons. Additionally, they identified structural elements that appear to be responsible for the onset of AD. Specifically, the areas of the brain where AD has a large impact on communicability distance. The majority of them connect the vermis or both hemispheres of the brain. In the same year, Paolo et al. [5] studied the mesoscale structure of the World Trade Network, identifying clusters using vibrational communicability distances and Estrada distances. The approach is more computationally efficient than traditional clustering techniques, identifies unique country links, and reveals inter and intra-cluster features.

On the other hand, as we explained in our recent paper [33], the hyperbolic space is a suitable space to study and understand the underlying dynamics of these financial networks. Specifically, we showed that the hyperbolic geometry enhances the clustering performance, using statistical analysis over the hyperbolic distance and the hyperbolic shortest path distance able to segregate the periods of volatility and stability and capture market trends earlier than the other traditional methods. The previous studies of the complex network following the heterogeneous degree distribution in the hyperbolic space also support the idea that the underlying geometry of the network boosts the capability of the network-based algorithms to capture the hidden structure of the system [8, 26]. In particular, the coalescent embedding techniques have been very popular, and embedding complex networks in hyperbolic spaces has several applications in the biology field. This algorithm uses the network power-law property to efficiently embed the complex network in the hyperbolic space.

In the present manuscript, we used the five-year dataset of the NIFTY 500 Index from the National Stock Exchange (NSE), India. The first step of our analysis is to model the stock market data as a complex network by considering pairwise correlations between stocks. It is worth noting that the full correlation-based network has a homogeneous degree distribution and, hence, does not obey the power law. Thus, we need to work with certain sub-graphs of the full network. The Minimum Spanning Tree (MST) and the Planar Maximally Filtered Graph (PMFG) have been popular models to explore in a huge body of research over the years [1, 13, 17, 24, 28, 29, 35, 37, 38]. In our previous work [33], we have already established that these subgraphs follow the power-law degree distribution. Furthermore, in this manuscript, we will be restricting our analysis over the PMFG network because this maintains several pathways, maintains structural complexity, and facilitates communication to capture indirect interactions, network resiliency, and realistic dynamics, providing deeper insights into network behaviour.

Next, we begin our analysis to determine how well the communicability network measure distinguishes the periods of market stability and volatility. Thus, we used the shortest path-based measures, namely edge betweenness centrality, shortest path length and along with communicability measure, as Features in the support vector machine (SVM) [16] in order to investigate how well it classifies the market periods. The results show that statistically, communicability is more sensitive to periods of volatility than the shortest path length of the financial network. Additionally, these network metrics edge betweenness centrality, shortest path length and communicability individually are able to classify the market periods of volatility using features in the SVM classifier with 95% accuracy. Furthermore, we used the SVM classifier on the geometry-based metrics of the embedded network in the hyperbolic space. The results suggest that, indeed, those geometric measures perform better than those that use only network topology.

There are five sections in this paper. First, we describe the data we utilized in our analysis in section

2. Our study's initial definitions and methodology are presented in Section 3. Section 4 provides the methods used for the several analyses that were conducted. The results are discussed in depth in Section 5. Lastly, we highlight our main findings and the work's implications for the future in the concluding section.

2. Data description

Our dataset contains the daily closing prices of all 500 stocks listed on the National Stock Exchange (NSE) India's NIFTY500 index between January 1, 2017, and December 31, 2021. This accounts for 1236 working days. We filtered the 117 stocks because of missing data on prices. This leaves us with the complete data of 383 stocks. Next, we calculate the daily logarithmic returns $r_i(t) = \log(p_i(t+1)) - \log(p_i(t))$. Here, $p_i(t)$ stands for the closing price of the stock i^{th} on day t . During this, we remove the data corresponding to non-successive days (like Friday & Monday are separated by more than 1 day due to holidays in between. Thus, we ignore the log return for Monday, and similarly, there were other exceptions also because of bank holidays). This provides us with 939 logarithmic return values corresponding to the above 383 stocks.

3. Methods and preliminaries

In this section, we first discuss the correlation-based network formulation using the above dataset. Then, we provide a brief overview of traditional complex network measures such as edge betweenness centrality, degree, Local clustering coefficient, eigenvector centrality, shortest path length, and communicability measure. In addition, we provide an overview of the algorithmic procedure of the permutation test, which we used to capture the significant stock pairs in the financial markets during significant market events. Furthermore, we provide a clear explanation of SVM and the method we used to classify stable and volatile market periods.

First, we begin by introducing the market metric, which is a correlation-based distance metric. Let $r_i(t)$ be the daily logarithmic price return at time t of the indices $i = 1, 2, 3, \dots, N$ where N is the total number of stocks. The time spans $t = 1, 2, 3, \dots, T$ where $T = 939$ is the maximum time of the data set. The person correlation coefficients (PCC) matrix $C = [C_{ij}]$ is defined as follows in terms of $r_i(t)$ as:

$$C_{ij} = \frac{E(r_i r_j) - E(r_i)E(r_j)}{\sqrt{E(r_i^2) - E(r_i)^2} \sqrt{E(r_j^2) - E(r_j)^2}} \quad (3.1)$$

Where $E(r_i)$ represents the expected value of returns corresponding to the i th stock.

$$D = [d_{ij}] = [\sqrt{2 * (1 - C_{ij})}] \quad (3.2)$$

We set the correlation distance between two stocks as defined above d_{ij} . The importance of using d_{ij} as a weight has been highlighted [4, 13, 17, 21, 28, 29, 34, 37, 38]. This distance is, in fact, equivalent to the Euclidean distance of the normalized return series.

In this paper, we worked with the weighted and unweighted Planar maximally filtered graph (PMFG) [38] and chose the weighted network representation as $G = (V, E, W)$, where V is the set of vertices (stock), E is the set of edges and W is the weighted adjacency matrix whose element w_{ij} is associated

to each edge in set E of the network. Thus, their weighted and unweighted adjacency matrices can be represented as

$$W = [w_{ij}] \text{ such that } w_{ij} = \begin{cases} C_{ij}, & \text{if } i \text{ and } j \text{ are adjacent} \\ 0, & \text{otherwise} \end{cases},$$

and

$$A = [a_{ij}] \text{ such that } a_{ij} = \begin{cases} 1, & \text{if } i \text{ and } j \text{ are adjacent} \\ 0, & \text{otherwise} \end{cases},$$

respectively. In the present manuscript, we consider the year 2018 to be a stable period and the year 2020 to be a period of volatility characterized by low and high standard deviation across the five-year dataset. Next, we construct the PMFG networks using the window of 60 days and one day as a sliding day. Therefore, there are 124 windows corresponding to the year 2018 and 137 corresponding to the year 2020.

3.1 Complex network measures

In this part, we give a brief overview of certain traditional network measures, such as shortest path length and edge betweenness. Finally, we provide a simple explanation of the measure of communicability between nodes in the network. In network science, numerous metrics are developed from the idea of shortest path length, which is defined as the number of edges in the shortest path [6] connecting nodes i and j . In weighted networks, the shortest path length is calculated as the sum of edge weights along the shortest path, where the shortest path length is the shortest cumulative edge weight among all potential pathways connecting the two nodes i and j .

Edge betweenness : The number of shortest paths that pass through an edge between two nodes is known as the edge betweenness [27]. This information indicates how crucial the relationship between two nodes is to the communication between all nodes in the network. A node's significance for the information flow throughout the network can be determined by applying the idea of betweenness to nodes as a measure of node centrality. Mathematically, the edge betweenness centrality $C_B(e)$ for an edge e in a graph is given by:

$$C_B(e) = \sum_{i \neq j \in V} \frac{\sigma_{ij}(e)}{\sigma_{ij}} \quad (3.3)$$

where:

- V is the set of vertices in the graph.
- σ_{ij} is the total number of shortest paths between vertices i and j .
- $\sigma_{ij}(e)$ is the number of shortest paths between i and j that pass through edge e .

Communicability Measure : The idea of communicability in a network is based on how a pair of nodes can communicate, namely, through walks connecting them. In usual settings, network measurements are based on the assumption that the information between two nodes travels over the shortest path, and communication between the two nodes is typically regarded as the shortest path. However, in many real-world networks, including Financial, biological, social and communication networks, information can travel down channels other than the shortest one, and it can flow back and forth numerous

times before arriving at its final destination. Indeed, especially in a network operating in a diffusion-like process, information does not always flow through the shortest paths because the sender may not know the network's global structure: (i) it may not know which of the many routes connecting it to the addressee is the shortest, and (ii) even if it knows the shortest path, it may not know whether there are damaged edges along this path. In the literature, two definitions of communicability have been introduced: Estrada Communicability and Vibrational Communicability [7, 15]. In this manuscript, we will restrict ourselves to Estrada Communicability [12]. Mathematically, it is defined between two nodes i and j of a network is defined as:

$$g_{ij} = \sum_{k=0}^{\infty} \frac{(A^k)_{ij}}{k!} = (e^A)_{ij} \quad (3.4)$$

Here, the (i, j) -entry of the k -th power of the adjacency matrix A represents the number of walks of length k starting at node i and ending at node j . The element g_{ij} encompasses all possible communication paths between two nodes, assigning greater significance to the shortest routes connecting them. It can also be understood as a measure of the probability that a particle, starting at node i , will arrive at node j after randomly traversing the complex network. This communicability matrix is denoted as g .

Further, in the case of a weighted network, communicability is defined as:

$$g_{ij} = \left(\exp \left(S^{-1/2} W S^{-1/2} \right) \right)_{ij} \quad (3.5)$$

where $S = \text{diag}(s_i)$ is the diagonal matrix whose diagonal entries are the strengths of the nodes (i.e. $s_i = \sum w_{ij}$). We will call this quantity-weighted communicability.

3.2 Coalescent Embedding Algorithm

In the year 2017, Muscoloni et al. introduced the coalescent embedding [26] technique that uses non-linear dimensionality reduction algorithms at its core. The dimensionality reduction is usually accomplished through popular algorithms like Isomap (ISO) (Tenenbaum et al., 2000), Non-centered Isomap (ncISO), Laplacian eigenmaps (LE) (Belkin and Niyogi, 2003), Minimum curvilinear embedding (MCE), and Non-centered minimum curvilinear embedding (ncMCE) (Cannistraci et al., 2010; Cannistraci et al., 2013). All these algorithms embed the weighted network (with weighted adjacency matrix \mathbf{W}) into the d -dimensional Euclidean space. However, these algorithms accept the distance between the nodes as input. Therefore, we convert the weight matrix into the corresponding distance matrix \mathbf{D} as:

$$\mathbf{D} = [d_{ij}] \text{ such that } d_{ij} = \begin{cases} \sqrt{2(1 - C_{ij})}, & \text{if vertex } i \text{ and } j \text{ are adjacent} \\ 0, & \text{otherwise} \end{cases},$$

and choose $d = 2$. The matrix \mathbf{D} is of order $N \times N$, and thus at this point, we have, for each vertex i , a pair of numbers (x_i, y_i) . Thus, next assign an angular coordinates defined as:

$$\theta_i = \tan^{-1} \left(\frac{y_i}{x_i} \right), \quad (3.6)$$

corresponding to each vertex. This approach of the angular assigned is referred to as the circular adjustment (CA). The second method of angular assignment is the equidistance adjustment (EA). For the i -th vertex it is defined by:

$$\theta'_i = \frac{2\pi}{N} (t_i - 1), \quad (3.7)$$

where t_i represents the rank assigned to the i -th vertex derived by sorting the original angular coordinates in ascending order.

Lastly, the radial coordinates were assigned to each vertex in the network. First, the vertex degrees are arranged in descending order $d_1 \geq d_2 \geq \dots \geq d_N$ (i.e., highest degree vertices appearing first). Then the radial coordinate for each $i = 1, 2, \dots, N$ is chosen as:

$$r_i = \frac{2}{\zeta} [\beta \ln(i) + (1 - \beta) \ln(N)]. \quad (3.8)$$

Where, $\beta = \frac{1}{\gamma-1} \in (0, 1]$ and γ is the power-law exponent. Thus, all the vertices of the network can, therefore, be represented by (r_i, θ_i) , and the above expression for r_i makes all of the vertices belong to the hyperbolic space. Also, in light of [10], the above adjustment to the radial coordinate forces the vertices to the hyperbolic space. For a detailed study regarding the equation, refer to [26, 31].

Further, we computed the those above-defined shortest path-based measures over the embedded networks in the Poincaré disc by choosing the edge weight between vertices i and j as follows:

$$w_{ij} = \frac{1}{1 + x_{ij}} \quad (3.9)$$

where x_{ij} is the hyperbolic distance between two nodes with polar coordinates (r, θ) and (r', θ') in the Poincaré disc is given by

$$x_{ij} = \frac{1}{\zeta} \cosh^{-1} (\cosh(\zeta r) \cosh(\zeta r') - \sinh(\zeta r) \sinh(\zeta r') \cos \Delta \theta) \quad (3.10)$$

where $\zeta = \sqrt{-K}$, we fixed $\zeta = 1$; K is the curvature of the hyperbolic space, and $\Delta \theta = \pi - |\pi - |\theta - \theta'||$ is the angular distance between the nodes. Thus, we denoted these hyperbolic geometry-based measures as Hebc, Hspl and Hcomm, and we will be using this notation to refer to them in the rest of the manuscripts. Note that in this paper, the results generated using the hyperbolic geometry-based measures are presented for the Isomap-CA class of the coalescent embedding algorithm since the results were similar for all other classes of the embedding.

3.3 Support vector machine algorithm

In the past years, support vector machine [2, 16] is a supervised learning algorithm that has been a very popular tool in solving the classification and regression problems in various domains, especially in computational biology, finance, and text categorization. In this manuscript, we used the Linear SVM with the aim of classifying the binary labels (+1 or -1). The main objective of the Linear SVM model is to find an optimal hyperplane that separates the two classes with the largest margin. The closet separation between the nearest +1 and -1 examples to a hyperplane is known as its margin. Because it should be more resilient and robust to noise than a hyperplane with a smaller margin, the hyperplane with the highest margin is chosen. For a given training dataset (x_i, y_i) for $i = 1, 2, 4, \dots, m$, such that $x_i \in \mathbb{R}$ feature vector and $y_i \in \{+1, -1\}$ are the class labels. Then learn a classifier that has a form

$$f(x) = w^T x + b, \quad (3.11)$$

where $w \in \mathbb{R}^d$ is the weight vector (normal to the hyperplane) and $b \in \mathbb{R}$ is the bias term, such that

$$f(x_i) = \begin{cases} +1, & w^T x_i + b \geq 0 \\ -1, & w^T x_i + b < 0 \end{cases} \quad (3.12)$$

i.e. $y_i f(x_i) > 0, \forall i$ for a correct classification. Further, we see that the value $\frac{b}{\|w\|}$, from the origin to hyperplane is the perpendicular distance, where this $\|w\|$ is the usual Euclidean norm. Next, we calculate the distance between the two separating hyperplanes that we say margin defined as $\frac{2}{\|w\|}$. Thus, the following problem can be solved to construct in order to get the largest margin that separates hyperplane: As an optimization problem that has form

$$M = \min_w \frac{1}{2} \|w\|^2 \quad (3.13)$$

subject to the constrains $y_i f(x_i) > 0, \forall i$. In the literature, this optimization problem is solved using the primal optimization approach and Lagrangian formulation.

3.4 Sensitivity analysis on communicability

The main objective of this study was to determine whether the communicability measure was a suitable metric to characterize the breakdown in communication between different pair stocks during the crisis or pandemic periods of the financial market. Therefore, we examine the sensitivity of the shortest communicability path length and shortest topological path lengths comparatively to detect significant changes in network connectivity during market crises. The procedure is outlined as follows:

1. Initially, for each connectivity matrix, we calculate both the shortest communicability path length matrix and the shortest topological path length matrix.
2. Next, for the statistical significance analysis, we use the permutation tests. Specifically, consider nodes x_i and x_j . Then compute the shortest communicability path length between these nodes for each window corresponding to the periods of Stability, denoted as l_{x_i, x_j}^S , and for each window corresponding to the periods of Volatility, denoted as l_{x_i, x_j}^V . Then, compute the respective average values as \bar{l}_{x_i, x_j}^S and \bar{l}_{x_i, x_j}^V . Furthermore, using these averages, then compute their difference :

$$\Delta l_{x_i, x_j} = \bar{l}_{x_i, x_j}^S - \bar{l}_{x_i, x_j}^V.$$

3. To assess significance, perform randomization of windows into two groups (stable and volatile periods): stability and volatility. Generate 1,000 random subsets for stability period windows and 1,000 random subsets for volatility period windows. Next, for each random subset, compute:

$$\Delta l_{x_i, x_j}^{\text{rand}} = \bar{l}_{x_i, x_j}^{\text{rand}, S} - \bar{l}_{x_i, x_j}^{\text{rand}, V},$$

where $\bar{l}_{x_i, x_j}^{\text{rand}, S}$ and $\bar{l}_{x_i, x_j}^{\text{rand}, V}$ are calculated similarly but using the randomized groups.

4. Further, we compare the null distribution of $\Delta l_{x_i, x_j}^{\text{rand}}$ with the true value $\Delta l_{x_i, x_j}$. A value $\Delta l_{x_i, x_j}$ for a node pair x_i and x_j is considered significant if it lies outside the central 95% of the null distribution. The p value is calculated using permutation testing to confirm its significance.
5. A node is considered to be significant if its p -value is less than 0.001.

3.5 Classification Analysis

The second objective of our investigation was to compare classification models trained using communicability versus models trained with standard metrics using the same dataset. Also, compare classification models trained using traditional network metrics versus models trained with network metrics obtained in the hyperbolic space. Linear support vector machines (SVMs) [16] were performed for the learning and classification process. First, we start with the calculation of the weighted and unweighted adjacency matrices for both the periods as explained above, and then we computed the network measures of the original correlation-based network as well as the embedded network in the hyperbolic space. The weight between the node in hyperbolic space is settled using the approach 3.9 referenced in [8, 26]. Further, we computed the topology-based measures (ebc, spl, comm) as well the geometry-based measures (Hebc, Hspl, Hcomm) as explained in the above sections. They are referred to as "connectivity measures" in the remainder of the text.

Next, we perform the following stage, which involves correctly dividing the dataset into training and test sets in order to validate the classification process. This was accomplished by performing a 10-fold cross-validation 50 times. This procedure involved splitting the entire set of examples into ten subsets, or folds: one fold served as the test set, and the remaining folds comprised the training set. This splitting procedure was repeated until every fold was utilized as a test set once. It is important to remember that all 261 windows were Labeled by their corresponding stable group or volatile group. Additionally, we shuffled the windows into the folds for a more general approximation of the performance by repeating the 10-fold cross-validation 50 times with various permutations.

Furthermore, we performed the two-stage feature selection methods that were used to reduce the dimensionality of the feature space and ease the over-fitting issue. An ad hoc feature selection process applied to weighted connectivity matrices. In order to minimize the number of links into the network that needed to be taken into account for classification, corresponding to the stable period, a binary mean matrix, or a mask, was calculated, onto which the matrices of all windows (both periods) were subsequently projected. The stable period mean matrix is a weighted matrix, where each entry e_{ij} ranges from 0 to 1 and indicates the frequency of the corresponding edge that occurs among all the stable period's connectivity matrices.

We then threshold this mean matrix in order to obtain the referenced stable period binary mean matrix and use it as a mask matrix. The threshold value was chosen at 0.6, using a binomial test (with $\alpha = 0.01$): if we consider a prior probability of 0.5 that a link is present or not in a connectivity matrix, the binomial test established that a link is considered to be an 'important' link if it occurs in more than 70 % of all stable periods connectivity matrices. These stable period connectivity matrices show a more stable topology; volatile periods connectivity matrices, instead, show a greater intra-variability due to the disrupted connectivity. This procedure would evaluate a significant and robust reference model to select the important links, as the sampling of windows considered in each round makes the definition of the set of significant links (i.e., the mask) robust with respect to outliers. Additionally, weak connections that can introduce noisy effects are filtered out in accordance with an objective statistical test with a strict significance threshold of the mask. This nested procedure of significant link selection was preferred to other threshold methods, such as fixing the same mean degree across all groups.

Using the feature matrices chosen in the first step, the second stage applied a traditional SVM recursive feature elimination (SVM-RFE) procedure [14, 22]. The criteria used by SVM-RFE to rank features are taken from the coefficients of linear SVM models that have been trained. The feature that has the least amount of influence on categorization, as shown by its lowest ranking criterion, is eliminated at each iteration. Iteratively, this procedure keeps on until every feature is ranked. By keeping the best-

ranked characteristics, feature selection is accomplished.

To address the underestimating of strongly correlated features, we applied the method in [42], which included a correlation bias reduction technique. In order to avoid feature selection bias and guarantee objective performance evaluation, a nested feature selection technique was used during cross-validation, in which the two-stage feature selection procedure was carried out only on the training set. An SVM model was trained to categorize data after dimensionality was decreased. The SVM algorithm uses its powerful generalization capabilities, which are especially useful in high-dimensional feature spaces, to find a separating hyperplane with the largest margin between classes. The summarized flow of this classification analysis is provided below in section 3.5.1.

3.5.1 *Algorithmic Steps for Classification Analysis*

Step 1: Networks construction and computation of connectivity measures

1. Extract data corresponding to Year 2018 and Year 2020 from the five-year dataset.
2. Construct the correlation network using a 60-day rolling window size and 1 day as a sliding day. This implies that there are 124 networks corresponding to the year 2018 (stable period) and 137 networks corresponding to Year 2020 (volatility period). Here, we also embed each 261 network in the Poincare disc, refer as embedded networks.
3. Compute the measure matrices (ebc, spl, comm) of each correlation network as well as the measure matrices of (Hebc, Hspl, Hcomm) the embedded network corresponding to both periods.
4. Construct the mean matrix (with threshold 0.6) using the 124 networks of the stable period as a mask matrix, onto which all the measure matrices of both periods are projected.
5. Further, flatten each of the measure matrices as a vector of length 73,153. Then there will be complete data of size $261 \times 73,153$.

Step 2: Shuffle, reorder the windows and data Splitting

1. Create a list of indices and labels (+1 as stable Windows 2018 and -1 as volatile Windows 2020), and shuffle them randomly while keeping labels aligned.
2. Use shuffled indices to reorder the 261 windows of step 1.5 with labels.
3. Normalize data distribution and split the dataset into training (80%) and testing (20%).

Step 3: Feature Extraction using Recursive Feature Elimination

1. Begin with the SVM classifier and use the linear kernel.
2. Extract the top 50 significant features using Recursive Feature Elimination.
3. Next, train the SVM on the training data using selected features.
4. Further, Use the test dataset to assess the trained model's classification performance.

Step 4: Cross-Validation with performance measures

1. Perform repeated stratified k-fold cross-validation (5 splits, 10 repeats).

2. Compute accuracy and AUC (Area Under Curve) scores.
3. For each fold: First, train the model and get the predictions. then Calculate the confusion matrix in order to calculate the sensitivity and specificity.
4. Compute the accuracy, AUC, sensitivity, and specificity by calculating the mean and standard deviation. then compare them by plotting the findings in a bar chart.

4. Results

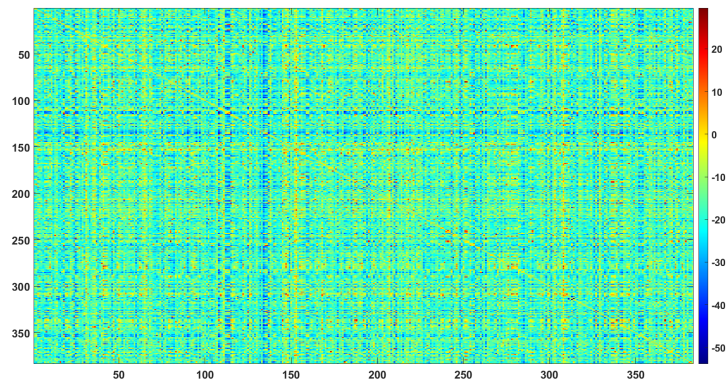
The findings of the statistical analysis on communicability and SVM classification are described in the following subsections.

4.1 *Statistical Differences in communicability*

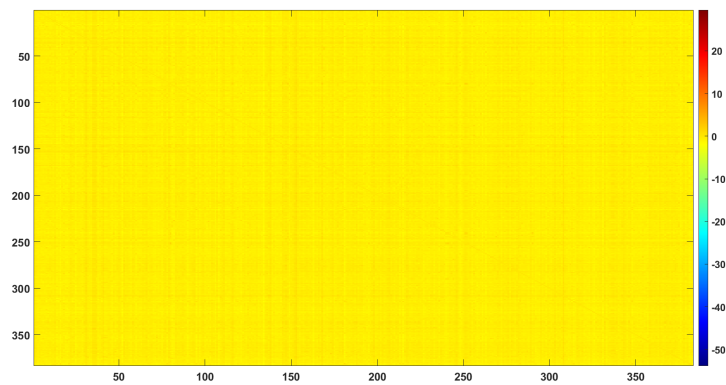
First, we computed the average shortest communicability path length matrix for both the periods of stability and volatility. Next, we have derived the difference between the matrix corresponding to the stability periods and volatility periods provided as heat map Figure 1 (a). We also calculated these differences for the shortest path lengths between each pair of nodes for comparison's sake Figure 1 (b). The differences for the shortest topological path length were set at the same scale as the differences of the shortest communicability path length, and we represented these differences using a diverging colour map centre at zero. From these figures, one can see that the communicability path length is more sensitive to enhanced connectivity in the stock pairs than the shortest path length. Notably, we observed in the communicability difference heat map that the average shortest communicability path length of most of the banking stocks, such as AXISBANK, PNB, ICICIBANK, SBIN, and BOBANK, is positive with most of the other stocks than the communicability between the other stock pairs, suggesting that these stocks are used more frequently than others for the communication of market information in the stock market during the periods of crisis. Thus, it also aligns with the usual theory of the market.

Further, we considered the stable and volatile periods windows as two separate groups and used the procedure outlined in section 3.2 for using the permutation test. we found around (83.5% of the total distinct pairs) distinct stock pairs were found to have statistically significant different communicability (adjusted $P < 0.001$). Most of these significant stock pairs showed an increased average communicability in the volatile period. Looking at the stable and volatile period distributions Figure 2 (a) of the average communicability values of all these significant stock pairs, the hypothesis of a greater population median in the volatile period was tested by performing a one-sided Wilcoxon rank sum test [43]. A P-value of 0 was obtained: with enough evidence, it can be concluded that there is a positive shift in the median of the average communicability values of the significant edges (or stock pairs) in the volatile period compared with the stable period at the 0.001 significance level, pointing out an overall communicability amplification between the stock pairs due to volatility of the stock market. Notable Observation: A prominent starting tail on the left side of the year 2020 indicates a subset of data points (stock pairs) that have much lower average communicability. This shows the presence of abnormalities or disturbances in network connectivity throughout the year, possibly due to the economic impact of a crisis such as COVID-19. while that was not purely clear in average shortest path length distribution Figure 2 (b).

The above analysis is performed for both the shortest communicability path lengths and the shortest topological path lengths.

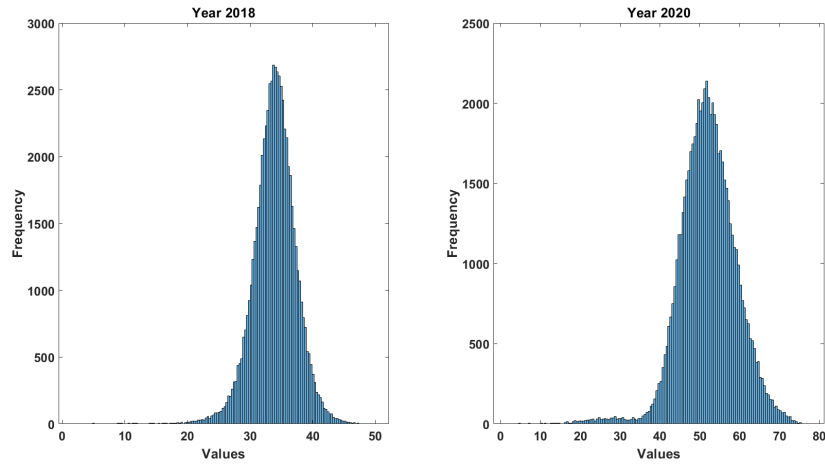


(a)

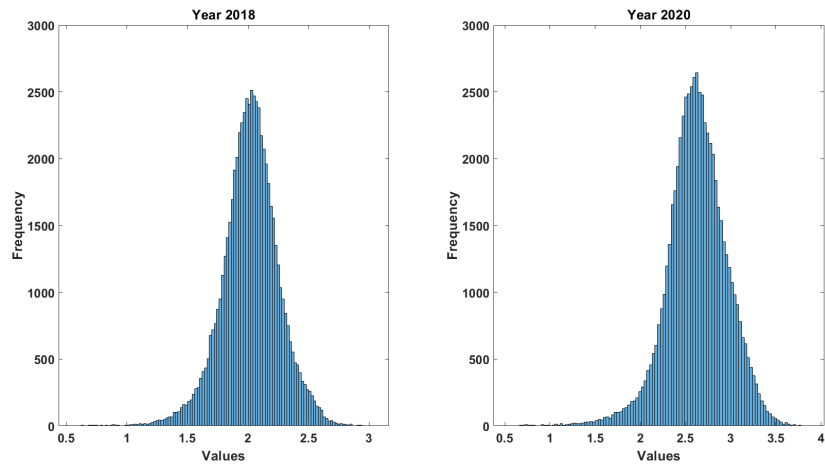


(b)

FIG. 1: (a) Heat map of the difference between the averaged shortest communicability path length for the periods of stability and volatility (b) Heat map of the difference between the averaged shortest topological path length for the periods of stability and volatility, on the same scale as (a). Both figures are generated using the unweighted adjacency matrices corresponding to both periods.



(a)



(b)

FIG. 2: (a) Histogram of the average shortest communicability path length in the stable period (the year 2018 and year 2020) corresponding to the significant stock pairs (b) Histogram of the average shortest topological path length in the volatile period (the year 2018 and year 2020) corresponding to the significant stock pairs. Both figures are generated using the weighted adjacency matrices corresponding to both periods.

4.2 Classification performance evaluation

We used the four natural performance measures, namely accuracy, sensitivity, specificity, and area under the ROC curve (AUC), to report the classification performances, which are averaged throughout all cross-validation rounds. Figure 3 summarizes the classification result attained with each network connectivity measure separately. The mean value derived from averaging the outcomes across all cross-validation iterations is represented by each performance metric. Each bar's height in the figure represents the average performance, while the error bars show the corresponding standard errors. Overall, each measure individually performs superbly for classification between the stable and volatile periods in both original correlation networks and the embedded hyperbolic network. It is notable that the spl and comm measures perform accurately in all four performance measures for the classification between the periods. In this figure 3, it is not much distinguishable between the performances of the original correlation-based network metrics and the hyperbolic network-based metrics.

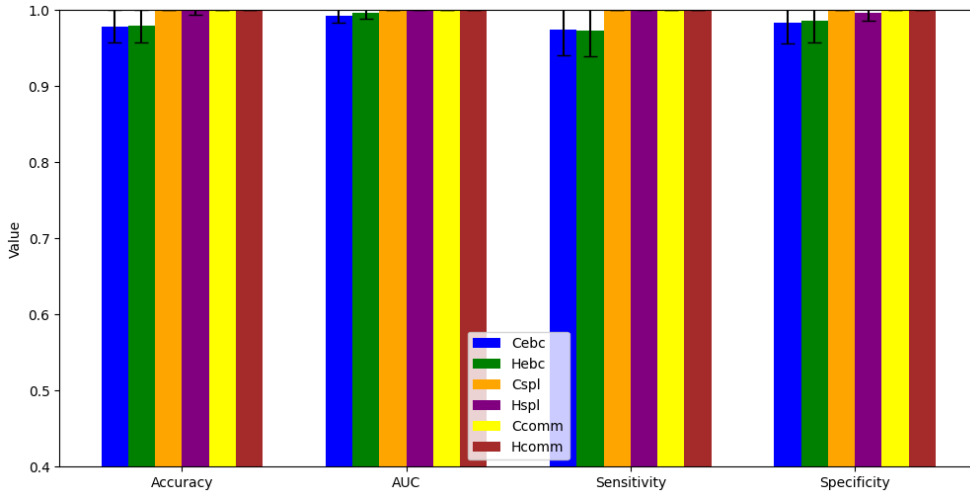


FIG. 3: Overview of the performances achieved by using, as features for the stable and volatile periods classification, the individual metrics computed on the weighted connectivity matrices.

Further, in order to assess the effectiveness of the communicability measure for the classification between these two periods, we experimented on the original correlation network measures *ebc* and *spl* together with or without communicability as features in SVM-RFE. Figure 4 shows that there is a bit of an effect on the performance after combining the communicability (*comm*) as a feature with the rest of the two measures, but not much better than their individual performances. It is quite acceptable that performance is approx 0.6 and above in all four performance measures in figure 4 for classification between these periods of volatility and stability.

A similar experiment was performed on the hyperbolic network measures (geometry-based measures) in order to see the effectiveness of hyperbolic communicability (*Hcomm*) together with or without two other network measures, *Hebc* and *Hspl*. We observe that the inclusion of Hyperbolic communicability, among the features used, significantly enhanced classification performances provided in Figure 5.

Finally, we performed an important analysis between all combined topology-based measures (ebc, spl, comm) and all combined geometry-based network measures (Hebc, Hspl, Hcomm) using as features in order to see their effectiveness in classification performance between the periods of stability and volatility periods. The related results are provided in figure 6. In this figure, we observe that the hyperbolic connectivity metrics outperformed all those topology-based metrics in terms of all four performance measures: accuracy, sensitivity, specificity, and area under the ROC curve (AUC).

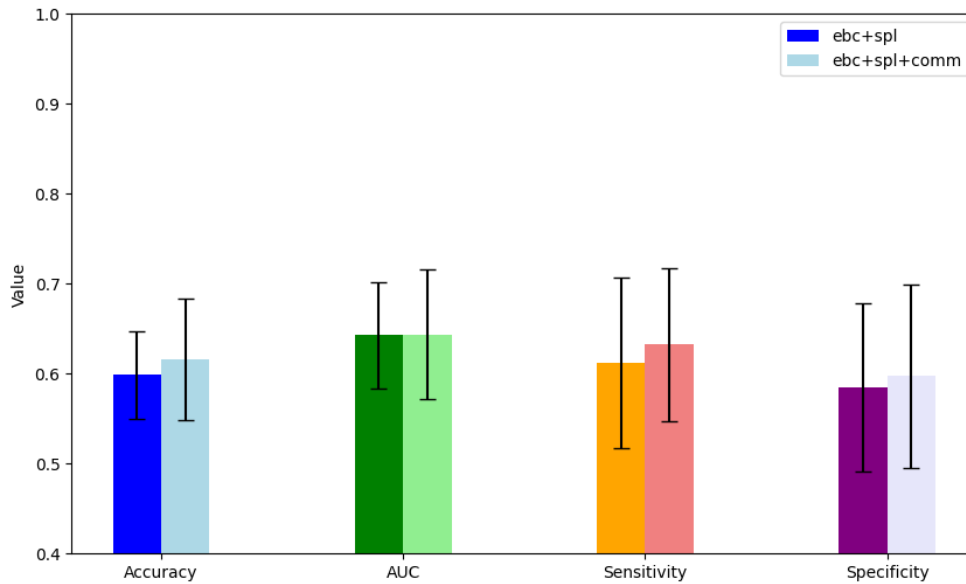


FIG. 4: Performance overview of all the connectivity measures, with and without communicability, computed on weighted connectivity matrices (stable and volatile periods classification).

5. Discussion

This study's objectives were to examine the financial correlation-based network and demonstrate how the communicability measure may be used to highlight changes in connectivity between stock pairs during a stock market crisis. The advantage of using this metric has been evaluated from two points of view:

- A statistical analysis pointed out that stock pairs have different communicability values during periods of volatile and stable.
- The first observation in the classification methodology demonstrates that the shortest path-based network measurements can almost precisely differentiate between periods of market stability and volatility.

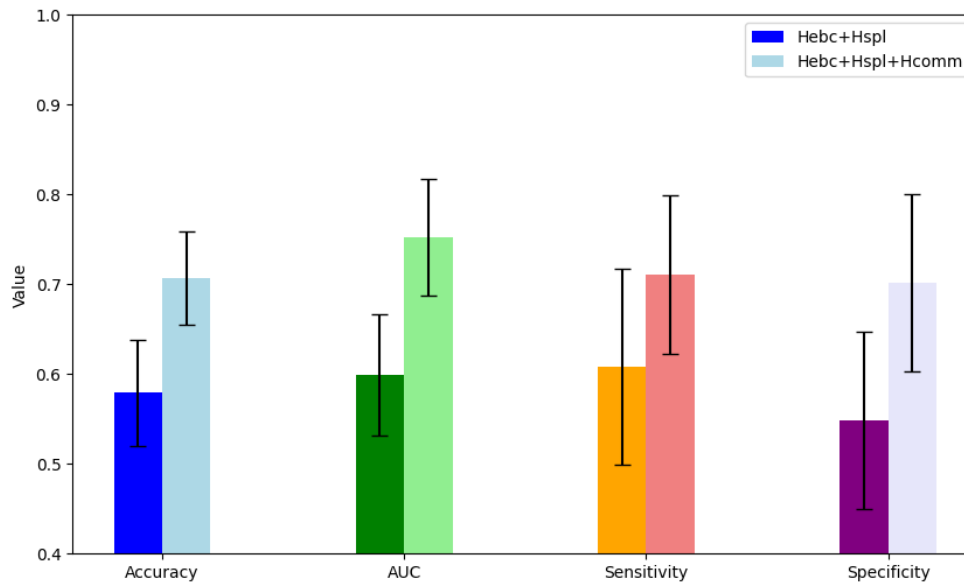


FIG. 5: Performance overview of all the hyperbolic connectivity measures, with and without community, computed on weighted connectivity matrices (stable and volatile periods classification)

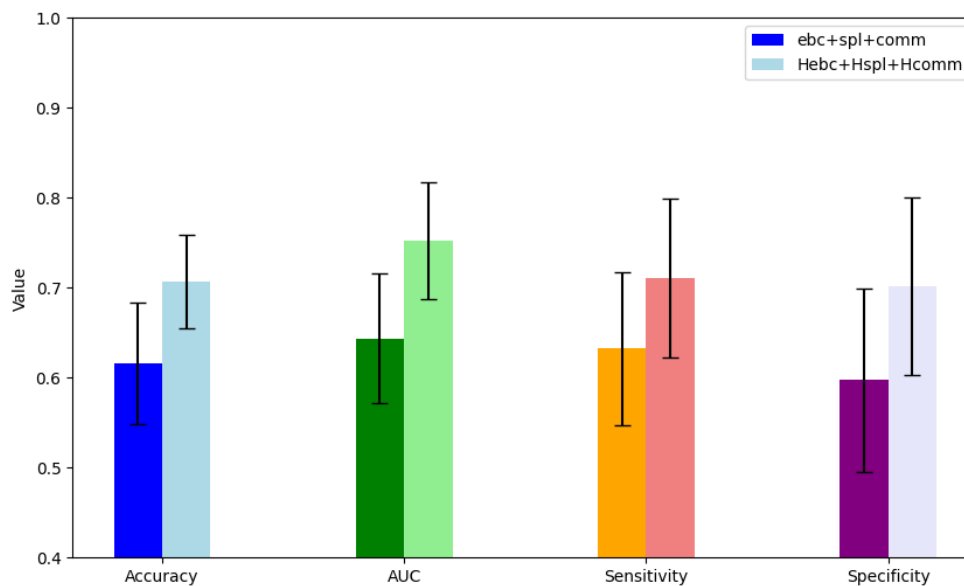


FIG. 6: Performance overview of all the connectivity measures versus the hyperbolic connectivity measures, computed on weighted connectivity matrices (stable and volatile periods classification)

- Secondly, the classification framework with binary groups of features showed how communicability positively affects classification performance both for the stable period/volatile period.
- The hyperbolic distance-based metrics outperformed the original correlation-based metrics in terms of classification robustness and accuracy. Furthermore, hyperbolic communicability has a greater favourable impact on classification performance than network topology-based communicability measures.

First, 83.5% stock pairs with statistically significant different communicability values between stable period and volatile period windows have been found. Second, in the classification scenarios, this study demonstrates that when features are incorporated in the classification model, the shortest path-based network measures and the communicability measure almost reliably distinguish between times of market stability and volatility. Furthermore, it has been demonstrated that in the financial system, communicability appears to be a more effective measure than those based on shortest paths. Finally, it was demonstrated that the geometry-based measures are more successful than the topology-based measures in classifying the market periods.

6. Conclusion

In this study, we explored the shortest path-based network measures along with the communicability measure in financial networks, and we were successfully able to discover the connectivity differences between the periods of stability and volatility in stock networks. Communicability can be considered an alternative measure to traditional ones that are mostly based on the shortest path length. In the first step, the importance of investigating a metric more suitable to describe diffusive processes was highlighted.

The use of communicability to network connectivity was initially examined in this study with a statistical-descriptive goal: stock pairs with statistically significant differences in communicability values during volatile and stable periods were identified. This indicates the enhanced connectivity and the heightened information flow between the stock pairs during the turbulence periods. Second, the advantage of applying communicability was investigated from a quantitative point of view: it was demonstrated that the classification tasks between the periods of stability and volatility, individually and along with the communicability measure as features for training the classification models. The study reports that the individual with this measure is able to classify these periods accurately, and the inclusion of the communicability measures improves the performances achieved using traditional network measures instead. Next, this study shows that the geometry-based measures of the network have greater classification capability than those network topology-based measures. The underlying geometry boosts the performance of these measures. The final goal of this article was to introduce a novel methodology in the classification analysis for the study of the stock network during different market conditions.

The efficiency of the communicability measures in uncovering connectivity differences between the two different stock market periods convinces us that communicability could be a powerful, distinguishing factor for a more accurate understanding of the market information dynamics. The use of the communicability measure in this context can represent a starting point for developing new classification strategies based on this measure that could further improve classification performance. The advantage of using communicability for this purpose is not limited to classifying the financial periods but can contribute to the early detection of the stock market crisis, which is one of the major challenges in current research in the finance system. In summary, this study combines machine learning, network science, hyperbolic geometry, and financial analysis to provide fresh and insightful perspectives on the crisis in the Indian stock market. It presents an approach that successfully classifies the periods of mar-

ket volatility from stability. furthermore, it showcases the superior classification performance of the geometry-based network measures. In the future, we will conduct this study in other foreign stock markets, such as the Shanghai and New York stock exchanges, to observe the consistency and robustness of this work outside of the Indian stock market.

Acknowledgments

We thank the Shiv Nadar Institution of Eminence for providing the computational resources and infrastructure required to conduct this research. We are very grateful to Professor Sanjeev Agrawal for his support and helpful comments. The first author thanks the Council of Scientific and Industrial Research (CSIR), India, Senior Research Fellowship Scheme (Grant No. 09/1128(12964)/2021-EMR-I) for financial assistance for this study.

REFERENCES

1. Ansari, I., Sharma, C., Agrawal, A. & Sahni, N. (2024) A novel portfolio construction strategy based on the core-periphery profile of stocks. *arXiv preprint arXiv:2405.12993*.
2. Apostolidis-Afentoulis, V. & Lioufi, K.-I. (2015) SVM classification with linear and RBF kernels. *July*: 0-7. [http://www.academia.edu/13811676/SVM_Classification_with_Linear_and_RBF_kernels.\[21\]](http://www.academia.edu/13811676/SVM_Classification_with_Linear_and_RBF_kernels.[21]).
3. Araújo, T. & Louçã, F. (2007) The geometry of crashes. A measure of the dynamics of stock market crises. *Quantitative Finance*, **7**(1), 63–74.
4. Aste, T., Shaw, W. & Di Matteo, T. (2010) Correlation structure and dynamics in volatile markets. *New Journal of Physics*, **12**(8), 085009.
5. Bartesaghi, P., Clemente, G. P. & Grassi, R. (2020) Community structure in the world trade network based on communicability distances. *Journal of Economic Interaction and Coordination*, pages 1–37.
6. Boccaletti, S., Latora, V., Moreno, Y., Chavez, M. & Hwang, D.-U. (2006) Complex networks: Structure and dynamics. *Physics reports*, **424**(4-5), 175–308.
7. Borgatti, S. P. (2005) Centrality and network flow. *Social networks*, **27**(1), 55–71.
8. Cacciola, A., Muscoloni, A., Narula, V., Calamuneri, A., Nigro, S., Mayer, E. A., Labus, J. S., Anastasi, G., Quattrone, A., Quartarone, A. et al. (2017) Coalescent embedding in the hyperbolic space unsupervisedly discloses the hidden geometry of the brain. *arXiv preprint arXiv:1705.04192*.
9. Crofts, J. J. & Higham, D. J. (2009) A weighted communicability measure applied to complex brain networks. *Journal of the Royal Society Interface*, **6**(33), 411–414.
10. Dorogovtsev, S. N., Mendes, J. F. F. & Samukhin, A. N. (2000) Structure of growing networks with preferential linking. *Physical review letters*, **85**(21), 4633.
11. Echaust, K. & Just, M. (2014) Geometry of crises on the market of stocks listed on the Warsaw stock exchange. *Studia Ekonomiczne*, **207**, 51–66.
12. Estrada, E. & Hatano, N. (2008) Communicability in complex networks. *Physical Review E—Statistical, Nonlinear, and Soft Matter Physics*, **77**(3), 036111.
13. Guo, X., Zhang, H. & Tian, T. (2018) Development of stock correlation networks using mutual information and financial big data. *PLoS one*, **13**(4), e0195941.
14. Guyon, I., Weston, J., Barnhill, S. & Vapnik, V. (2002) Gene selection for cancer classification using support vector machines. *Machine learning*, **46**, 389–422.
15. Hromkovič, J., Klasing, R., Pelc, A., Ruzicka, P. & Unger, W. (2005) *Dissemination of information in communication networks: broadcasting, gossiping, leader election, and fault-tolerance*. Springer Science & Business Media.
16. James, G., Witten, D., Hastie, T., Tibshirani, R. et al. (2013) *An introduction to statistical learning*, volume 112. Springer.

17. Jiang, X., Chen, T. & Zheng, B. (2014) Structure of local interactions in complex financial dynamics. *Scientific Reports*, **4**, 5321.
18. Keller-Ressel, M. & Nargang, S. (2021) The hyperbolic geometry of financial networks. *Scientific reports*, **11**(1), 4732.
19. Kukreti, V., Pharasi, H. K., Gupta, P. & Kumar, S. (2020) A perspective on correlation-based financial networks and entropy measures. *Frontiers in Physics*, **8**, 323.
20. Kulkarni, S., Pharasi, H. K., Vijayaraghavan, S., Kumar, S., Chakraborti, A. & Samal, A. (2024) Investigation of Indian stock markets using topological data analysis and geometry-inspired network measures. *Physica A: Statistical Mechanics and its Applications*, **643**, 129785.
21. Kumar, S. & Deo, N. (2012) Correlation and network analysis of global financial indices. *Physical Review E—Statistical, Nonlinear, and Soft Matter Physics*, **86**(2), 026101.
22. Lella, E., Amoroso, N., Lombardi, A., Maggipinto, T., Tangaro, S., Bellotti, R. & Initiative, A. D. N. (2019) Communicability disruption in Alzheimer’s disease connectivity networks. *Journal of Complex Networks*, **7**(1), 83–100.
23. Lella, E. & Estrada, E. (2020) Communicability distance reveals hidden patterns of Alzheimer’s disease. *Network Neuroscience*, **4**(4), 1007–1029.
24. MacMahon, M. & Garlaschelli, D. (2015) Community Detection for Correlation Matrices. *Physical Review X*, **5**(2).
25. Mendes, R. V., Araújo, T. & Louçã, F. (2003) Reconstructing an economic space from a market metric. *Physica A: Statistical Mechanics and its Applications*, **323**, 635–650.
26. Muscoloni, A., Thomas, J. M., Ciucci, S., Bianconi, G. & Cannistraci, C. V. (2017) Machine learning meets complex networks via coalescent embedding in the hyperbolic space. *Nature communications*, **8**(1), 1615.
27. Newman, M. E. & Girvan, M. (2004) Finding and evaluating community structure in networks. *Physical review E*, **69**(2), 026113.
28. Nie, C.-X. (2021) Studying the correlation structure based on market geometry. *Journal of Economic Interaction and Coordination*, **16**(2), 411–441.
29. Nie, C.-X. & Song, F.-T. (2018) Constructing financial network based on PMFG and threshold method. *Physica A: Statistical Mechanics and its Applications*, **495**, 104–113.
30. Onnela, J.-P., Saramäki, J., Kertész, J. & Kaski, K. (2005) Intensity and coherence of motifs in weighted complex networks. *Physical Review E—Statistical, Nonlinear, and Soft Matter Physics*, **71**(6), 065103.
31. Papadopoulos, F., Kitsak, M., Serrano, M. Á., Boguná, M. & Krioukov, D. (2012) Popularity versus similarity in growing networks. *Nature*, **489**(7417), 537–540.
32. Pawanesh, P., Ansari, I. & Sahni, N. (2024a) Exploring the core-periphery and community structure in the financial networks through random matrix theory. *arXiv preprint arXiv:2410.07947*.
33. Pawanesh, P., Sharma, C. & Sahni, N. (2024b) Exploiting the geometry of heterogeneous networks: A case study of the Indian stock market. *arXiv preprint arXiv:2404.04710*.
34. Pozzi, F., Di Matteo, T. & Aste, T. (2013) Spread of risk across financial markets: better to invest in the peripheries. *Scientific reports*, **3**(1), 1665.
35. Purqon, A. & Jamaludin (2021) Community Detection of Dynamic Complex Networks in Stock Markets Using Hybrid Methods (RMT-CN-LPAm+ and RMT-BDM-SA). *Frontiers in Physics*, **8**, 574770.
36. Samitas, A., Kampouris, E. & Kenourgios, D. (2020) Machine learning as an early warning system to predict financial crisis. *International Review of Financial Analysis*, **71**, 101507.
37. Sharma, C. & Habib, A. (2019) Mutual information based stock networks and portfolio selection for intraday traders using high frequency data: An Indian market case study. *PloS one*, **14**(8), e0221910.
38. Tumminello, M., Aste, T., Di Matteo, T. & Mantegna, R. N. (2005) A tool for filtering information in complex systems. *Proceedings of the National Academy of Sciences*, **102**(30), 10421–10426.
39. Vilela Mendes, R., Lima, R. & Araújo, T. (2002) A process-reconstruction analysis of market fluctuations. *International Journal of Theoretical and Applied Finance*, **5**(08), 797–821.
40. Watts, D. J. & Strogatz, S. H. (1998) Collective dynamics of ‘small-world’ networks. *nature*, **393**(6684), 440–442.

41. Xiu, Y., Wang, G. & Chan, W. K. V. (2021) Crash diagnosis and price rebound prediction in NYSE composite index based on visibility graph and time-evolving stock correlation network. *Entropy*, **23**(12), 1612.
42. Yan, K. & Zhang, D. (2015) Feature selection and analysis on correlated gas sensor data with recursive feature elimination. *Sensors and Actuators B: Chemical*, **212**, 353–363.
43. Zar, J. H. (1999) *Biostatistical analysis*. Pearson Education India.